# Next-generation all-solid-state battery (#ASSB @ #OBMS23)

Tuan Vo<sup>a,b†</sup>, Claas Hüter<sup>b</sup>, Stefanie Braun<sup>a</sup>, Manuel Torrilhon<sup>a</sup>

<sup>a</sup>Department of Mathematics, Applied and Computational Mathematics (ACoM), RWTH Aachen University, Schinkelstraße 02, 52062 Aachen, Germany <sup>b</sup>Institute of Energy and Climate Research (IEK-2), Forschungszentrum Jülich, Wilhelm-Johnen-Straße, 52428 Jülich, Germany

### Mathematical modelling for the next-generation All-solid-state batteries: Nucleation (SE|SSE)(\*)-interface

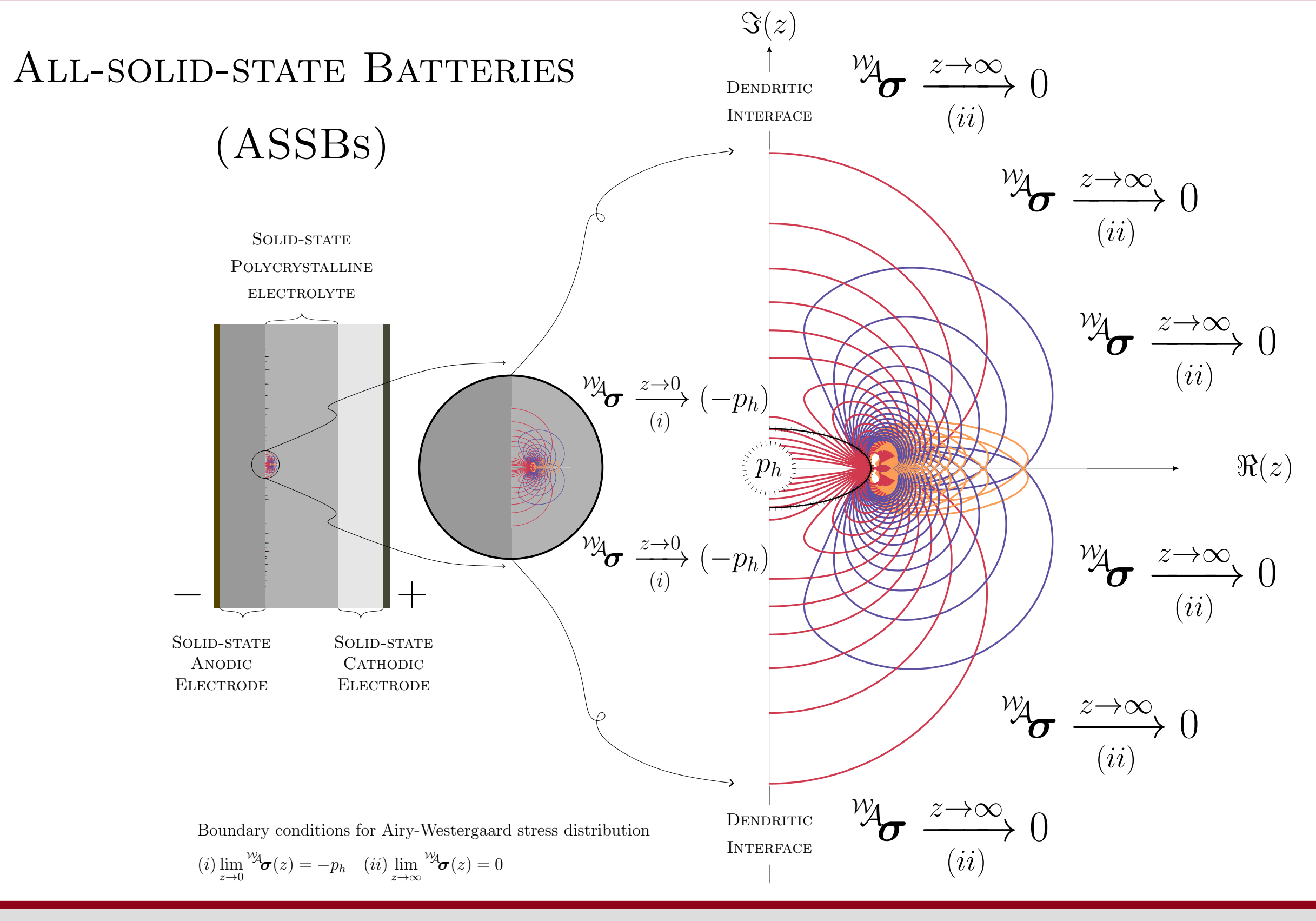
Rechargeable Lithium-ion battery (LIB) is at the heart of every electric vehicle (EV), portable electronic device, and energy storage system [1]. Nowadays, LIBs enable human life more efficient and help to solve global environment issues thanks to EVs' zero However, conventional LIB (c-LIB) is sensible to temperature and pressure, hence, flammable and explosive, which is undesirable. This bottleneck is mainly due to liquid-based electrolyte found in c-LIBs.

**All-solid-state battery** (ASSB) is one of promising candidates to overcome bottlenecks of c-LIBs. Thanks to solid-state electrolyte (SSE), ASSB is highly stable towards temperature and pressure. Nevertheless, Limetal dendrite triggered at (SE|SSE)-interface [5] is the main drawback of ASSB since these dendritic threads extrapolate into SSE grain boundary network, causing crevice, degradation of ionic conductivity, and the probability of short-circuit, which is unfavorable.

Next-generation All-solid-state battery (ng-ASSB) with a consideration of nucleation criterion defined by

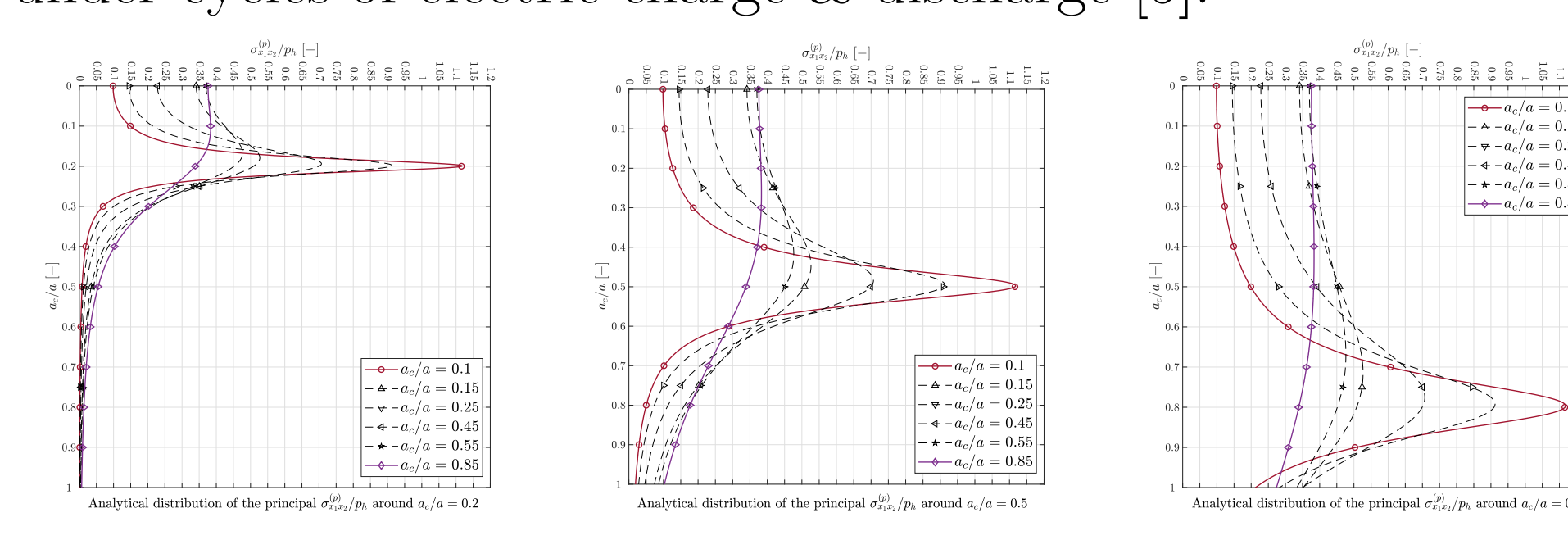
$$a_{\text{Griffith}} := a^* = \arg\min_{a \in \mathbb{R}} \left. \iint_{\Omega} f(a, \boldsymbol{u}, \theta; \lambda, \mu, \boldsymbol{d}^R \otimes \boldsymbol{d}^R) \, d\Omega - \left. \iint_{\Gamma} f(a; \gamma) \, d\Gamma \right|_{\boldsymbol{u}^{(s)}}$$

where  $\boldsymbol{u}$  displacement field,  $\theta$  temperature field, a crevice length,  $\lambda, \mu$  Lamé constants,  $\boldsymbol{d}^R \otimes \boldsymbol{d}^R$  embedded misorientation structural tensor, and  $\gamma$  cracking-surface energy density, can help to improve ASSB performance.



#### Interface Analysis

Interface between solid electrode and solid-state electrolyte (SE|SSE) taking place at space charge layer (SCL) [2] found in ASSBs critically exhibits mechanical and electrochemical instability [3]. This evidence points directly to the fact that the soft metallic li anode is erroneously prone to triggering dendrites, under cycles of electric charge & discharge [5].



<u>Distribution</u>: ana. max. shear stress  ${}^{\mathcal{W}}\!\!\sigma_{x_1x_2}^{\Pi}$  around crack tip  $a_c$ .

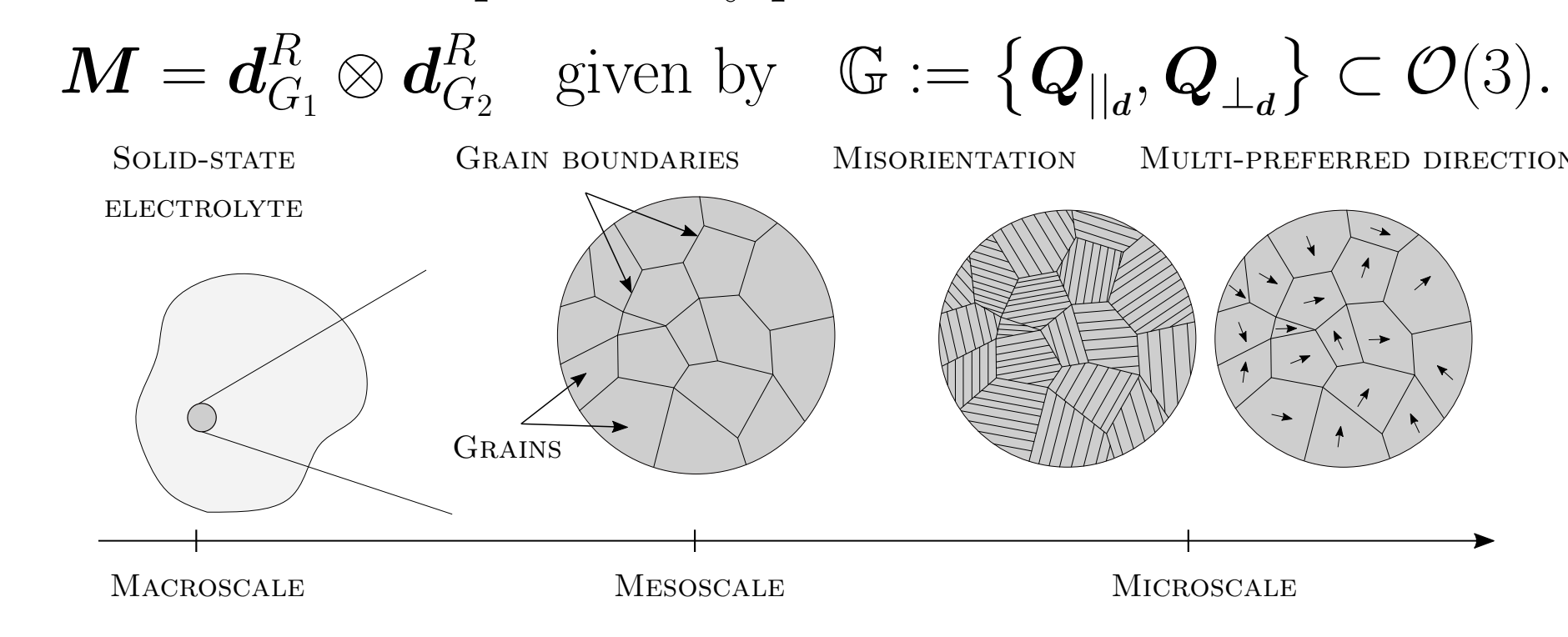
#### Next-generation All-solid-state battery

**Nucleation** criterion governs the instable (SE|SSE)-interface [3] COLLECTOR COLLECTOR ELECTROLYTE metal-oxide • e<sup>-</sup> — space charge layer — dendrite

**Thermodynamic consistency** is satisfied, followed by [2]. ✓ Closure  $\bar{\Omega}$  is fulfilled by 15 moments, followed by [4].

#### Embedded structural-tensor in SSE

Polycrystalline garnet-type SSE [5] such as LLZO exhibit grain boundary network, and grains with variation of (size, shape) under microscopic observation. Hence, this microstructure is potentially prone to nuances of destruction.



Consequentially, dendrites contribute to degradation of ionic conductivity and tiny-cracks tracing along grain boundaries.

#### Nucleation interface: Taking place at the critical dendritic interface

(a) Case 1

Coupled fields: Displacement field u and temperature field  $\theta$ ; structural tensor M

$$oldsymbol{u}: egin{cases} \Omega imes \mathbb{R}_{+} 
ightarrow \mathbb{R}^{3}, \ (oldsymbol{x}, t) \mapsto oldsymbol{u}(oldsymbol{x}, t), \end{cases} \quad heta: egin{cases} \Omega imes \mathbb{R}_{+} 
ightarrow \mathbb{R}, \ (oldsymbol{x}, t) \mapsto oldsymbol{\theta}(oldsymbol{x}, t), \end{cases} \quad oldsymbol{M}_{i=1,...,N}^{\{RR,RE\}}: egin{cases} oldsymbol{d}_{\text{Grain i}}^{R} \otimes oldsymbol{d}_{\text{Grain i}}^{R} \\ oldsymbol{d}_{\text{Grain i}}^{R} \otimes oldsymbol{d}_{\text{Grain i}}^{R} \end{cases}$$

Governing conservation equations

$$\frac{d}{dt} \int_{\Omega} (\cdot) \ d\Omega = \int_{\Omega} (\cdot)^{\text{action}} \ d\Omega + \int_{\partial \Omega} (\cdot)^{\text{action}} \ d\partial\Omega + \int_{\Omega} (\cdot)^{\text{production (+/-)}} \ d\Omega$$

used to describe balance of mass, conservation of linear momentum, conservation of angular momentum, and conservation of energy with  $\rho(\boldsymbol{x},t)$  is mass density per unit volume (puv);  $\boldsymbol{b}(\boldsymbol{x},t)$  body force puv;  $\boldsymbol{v}(\boldsymbol{x},t)$  velocity;  $e(\boldsymbol{x},t)$  internal energy puv; q(x,t) heat flux; r(x,t) heat source puv;  $\sigma$  Cauchy stress and  $\varepsilon$  infinitesimal strain. Then, the governing partial differential equation (PDE) of deformation takes the form

$$\partial_t oldsymbol{u} + 
abla \cdot \left( \overset{4}{\mathbb{C}}^{f_{ ext{alocation}}(\lambda, \mu, oldsymbol{d}_{G_i, i=1,...,N}^R, oldsymbol{d}^E; oldsymbol{x})} : 
abla oldsymbol{u}^{(s)} 
ight) + 
ho oldsymbol{b} = -
ho 
abla V_e,$$

where  $V_e: \mathbb{R}^3 \to \mathbb{R}$  is the electric potential applied globally on ASSB. Due to nature setting of ASSB taking the form (SE|SSE|SE) the electric potential becomes uniform.

Strain **energy** is based on the deformation of SSE due to dendrite formation at (SE|SSE)-interface

 $\iiint_{\Omega} f(a, \boldsymbol{u}; \lambda, \mu, \boldsymbol{d} \otimes \boldsymbol{d}) d\Omega$ 

Surface energy is analysized based on the open crevice cracking at (SE|SSE)interface affected by prescribed pressure

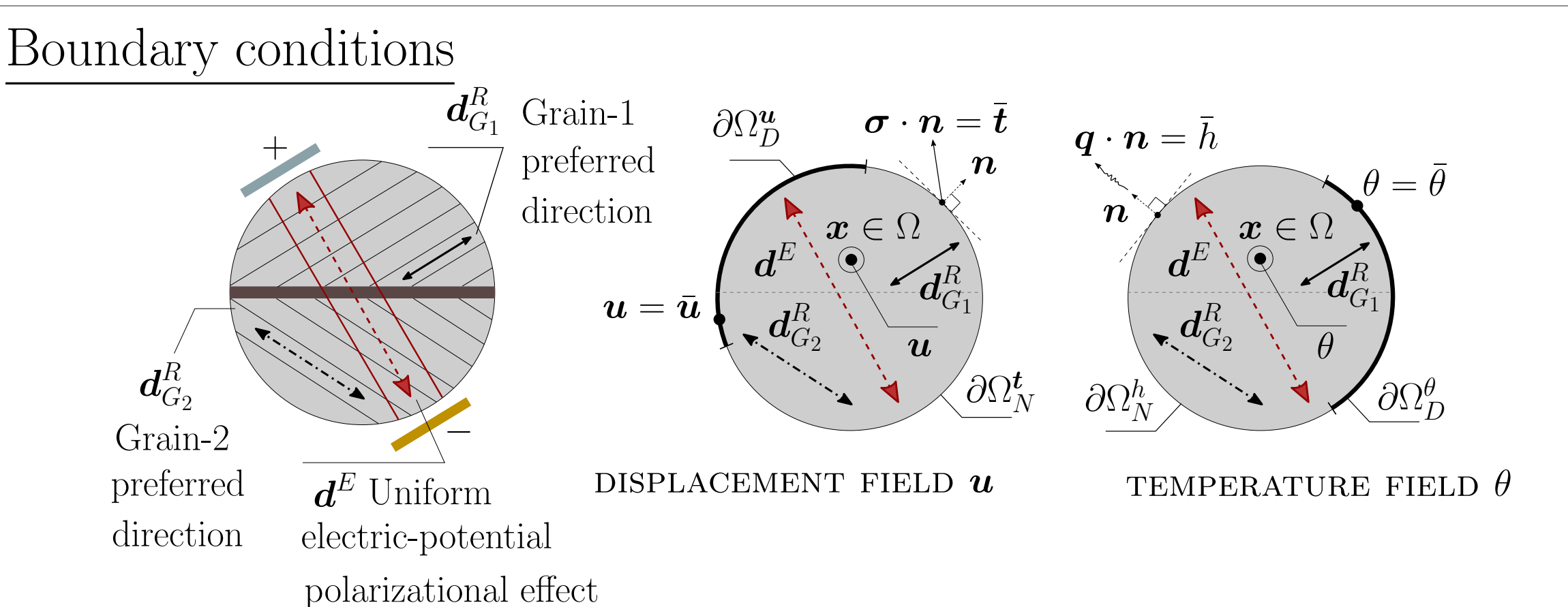
$$\iint_{\Gamma} f(a;\gamma) \, d\Gamma$$

Therefore, the governing problem of dendritic nucleation at (SE|SSE) takes the form

$$\partial_t \boldsymbol{u} + \nabla \cdot \left( \mathbb{C}^{f_{\text{alocation}}(\lambda, \mu, \boldsymbol{d}_{G_i, i=1, \dots, N}^R, \boldsymbol{d}^E; \boldsymbol{x})} : \nabla \boldsymbol{u}^{(s)} \right) + \rho \boldsymbol{b} = -\rho \nabla V_e, \tag{1}$$

s.t. 
$$a_{\text{Griffith}} := a^* = \arg\min_{a \in \mathbb{R}} \iiint_{\Omega} f(a, \boldsymbol{u}, \theta; \lambda, \mu, \boldsymbol{d} \otimes \boldsymbol{d}) d\Omega - \iint_{\Gamma} f(a; \gamma) d\Gamma \Big|_{\bar{\boldsymbol{u}}}$$
 (2)

where deformation  $\bar{\boldsymbol{u}}$  is (i) based on (1), and then (ii) for Griffith-analysis in (2).



Numerical spectral of Griffith criterion in x-direction at (SE|SSE) yields

 $a_{\text{crevice}} = 0.5$  $a_{\text{crevice}} = 0.3$  $a_{\text{crevice}} = 0.1$  $a_{\text{crevice}} = 0.01$  $a_{\text{crevice}} = 0.05$ where a sample of 5 cases with various prescribed crevice length is studied.

(c) Case 3

Partial differential equation (PDE)  $abla \cdot \left( \overset{4}{\mathbb{C}} f^{\mathbb{D}(\Omega)}_{(\lambda,\mu)} \, 
abla^{(s)} oldsymbol{u} 
ight) + 
ho \, oldsymbol{b} = oldsymbol{0}$ Displacement vector field solution  $oldsymbol{u_i} \leftarrow oldsymbol{u} = oldsymbol{K}^{-1} oldsymbol{f}$ Strain tensor  $arepsilon_{ij} = rac{1}{2} \left( \partial_{x_j} u_i + \partial_{x_i} u_j 
ight)$ Stress tensor  $\sigma_{ij} = \sum_{k,l} \overset{4}{\mathbb{C}}_{(\lambda,\mu)}^{f_{(\lambda,\mu)}^{\mathbb{D}(\Omega)}} \, arepsilon_{kl}$ Strain energy density  $\mathcal{E}_{ ext{strain}} := rac{1}{2} \sum_{i,j} oldsymbol{\sigma_{ij}} \, arepsilon_{ij}$ Strain solution takes the following form  $\frac{1}{2} \sum_{\alpha=1}^{\mathcal{N}_{\text{node}}^{\Omega^e}} \left( \sum_{L=1}^{\mathcal{N}_{\text{dof}}^{\Omega^{\text{node}}}} N_{,\xi_L}^{\alpha} \xi_{L,x_k} \boldsymbol{u}_k^{\alpha} + \sum_{K=1}^{\mathcal{N}_{\text{dof}}^{\Omega^{\text{node}}}} N_{,\xi_K}^{\alpha} \xi_{K,x_l} \boldsymbol{u}_l^{\alpha} \right)$ 

FEM: Strain energy density

Analysis: Airy-Westergaard function used for stress analysis: (i) max. shear stress and (ii) principal stresses

(d) Case 4

(e) Case 5

$$\mathcal{A}: \begin{cases} \mathbb{C} \to \mathbb{C}, \\ z \mapsto \mathcal{V} \mathcal{A}(z) := \Re(\iint_{\Gamma} \mathcal{K}^{(\star)} dz) + x_2 \Im(\oint_{\Gamma} \mathcal{K}^{(\star)} dz), \end{cases} \quad \mathcal{K}^{(\star)}: \begin{cases} \mathbb{C} \to \mathbb{C}, \\ z \mapsto \mathcal{K}^{(\star)} := -p_h + p_h/\sqrt{1 - a^2/z^2}, \end{cases}$$

where a the crevice length,  $p_h$  pressure at the opening crevice on dendritic interface, and  $\forall \{p_h, a\} \in \mathbb{R}_+$ .

<u>Numerics</u>  $\rightarrow$  <u>FEM</u>: element matrix  $\mathbf{K}^e$  approx. by *Gauss quadrature*; indices imply 4 + 2 = 6 for-loop:  $K_{ik}^{e^{\alpha\beta}} = \int_{\Omega^{\epsilon}} \left( \mathcal{L}_{1}^{\alpha} \, \mathbb{C}_{i1k1}^{f^{GL}}(\boldsymbol{x}) \, \mathcal{R}_{1}^{\beta} + \mathcal{L}_{1}^{\alpha} \, \mathbb{C}_{i1k2}^{f^{GL}}(\boldsymbol{x}) \, \mathcal{R}_{2}^{\beta} + \mathcal{L}_{2}^{\alpha} \, \mathbb{C}_{i2k1}^{f^{GL}}(\boldsymbol{x}) \, \mathcal{R}_{1}^{\beta} + \mathcal{L}_{2}^{\alpha} \, \mathbb{C}_{i2k2}^{f^{GL}}(\boldsymbol{x}) \, \mathcal{R}_{2}^{\beta} \right) \det(\boldsymbol{J}) \, d\Omega^{\xi}$ 

where  $\mathcal{L}_{i}^{\alpha}$  and  $\mathcal{R}_{l}^{\beta}$  are gradients of basis functions at node  $\alpha^{th}$  and  $\beta^{th}$ , respectively.

#### Contact

Tuan Vo vo@acom.rwth-aachen.de



## References

[1] **T.Vo**, Modeling the swelling phenomena of li-ion batt. cells based on a numerical chemo-mech. coupled approach. MA, Robert Bosch Battery Systems GmbH, **2018**.

(b) Case 2

[2] S.Braun, C. Yada and A. Latz, Thermodynamically consistent model for Space-Charge-Layer formation in a solid electrolyte. Ir. Phys. Chem., 119, 22281-22288, 2015.

[3] **C.Hüter**, S.Fu, M.Finsterbusch, E.Figgemeier, L.Wells, and R.Spatschek, *Electrode-electrolyte interface stability in solid state electrolyte system: influence of* coating thickness under varying residual stresses. AIMS Materials Science, 4(4):867-877, **2017**.

[4] **M.Torrilhon**. Modeling nonequilibrium gas flow based on moment equations. Annual Review of Fluid Mechanics, 48(1):429-458, **2016**.

[5] **S.Kim**, J.S.Kim, L.Miara, Y.Wang, S.K.Jung, S.Y.Park, Z.Song, H.King, M.Badding, J.M.Chang, V.Roev, G.Yoon, R.Kim, J.H.Kim, K.Yoon, D.Im, and K.Kang, High-energy and durable li metal batt. using garnet-type solid electrolytes with tailored li-metal compatibility. Nature Communications, 13(1):1883, 2022.









